Observation of new levels and proposed octupole correlations in neutron-rich ^{150}Ce

S. J. Zhu (□□□), M. Sakhaee, J. H. Hamilton, A. V. Ramayya, N. T. Brewer, J. K. Hwang, S. H. Liu, E. Y. Yeoh (□□□), Z. G. Xiao (□□□), Q. Xu (□□), Z. Zhang (□□), Y. X. Luo, J. O. Rasmussen, I. Y. Lee, K. Li, and W. C. Ma

Phys. Rev. C **85**, 014330 — Published 30 January 2012

DOI: 10.1103/PhysRevC.85.014330

Observation of new levels and proposed octupole correlations in neutron-rich ^{150}Ce

S. J. Zhu（朱胜江）,[1,2,*] M. Sakhaee,[1] J. H. Hamilton,[2] A. V. Ramayya,[2] N. T. Brewer,[2] J. K. Hwang,[2] S. H. Liu,[2,3] E. Y. Yeoh（杨韵颐）,[1] Z. G. Xiao（肖志刚）,[1] Q. Xu（徐强）,[1] Z. Zhang（张钊）,[1] Y. X. Luo,[2,4] J. O. Rasmussen,[4] I. Y. Lee,[4] K. Li,[2] and W. C. Ma[5]

[1]*Department of Physics, Tsinghua University, Beijing 100084, People's Republic of China*
[2]*Department of Physics, Vanderbilt University, Nashville, Tennessee 37235 USA*
[3]*UNIRIB/Oak Ridge Associated Universities, Oak Ridge, Tennessee 37831, USA*
[4]*Lawrence Berkeley National Laboratory, Berkeley, California 94720 USA*
[5]*Department of Physics and Astronomy, Mississippi State University, Mississippi State, Mississippi 39762, USA*

Background : The very neutron-rich ^{150}Ce is located at the edge of the Z = 56, N=88 octupole deformed island. To study its high spin states and octupole correlations is important for systematically understanding the nuclear structural characteristics in this region. **Purpose** : To investigate the high spin state levels and to search for octopole correlations in ^{150}Ce. **Methods** : The high spin states of ^{150}Ce are studied by measuring the prompt γ-rays in the spontaneous fission of ^{252}Cf. The data analysis is by using the γ-γ-γ coincidence methods. The $\gamma \rightarrow \gamma(\theta)$ angular correlation measurements are used to determine the spin and indirectly parity of particular levels. **Results** : A new level scheme of ^{150}Ce is established. A total of 47 new transitions and 25 new levels are identified comparing with previous results. Six collective bands have been observed and five of them are newly established. An octupole band structure with s = +1 in ^{150}Ce has been proposed. Systematic analysis for the B(E1)/B(E2) branching ratios, the levels of the octupole bands, the energy differences between negative- and positive-parity bands and the moments of inertia of the bands is carried out in ^{144,146,148,150}Ce. They give evidences for our assingment of octupole correlations in ^{150}Ce. The other characteristics of the octupole bands are discussed. **Conclusions** : An octupole band structure is proposed in ^{150}Ce. The octupole correlations in ^{150}Ce are weaker and show more instability than the neighboring lighter Ce isotopes.

PACS numbers: 21.10.Re, 23.20.Lv, 27.60.+j, 25.70.Jj

I. INTRODUCTION

In the study of nuclear structure, octupole deformation is a very important subject. A nucleus with octupole deformation has an asymmetric shape in its intrinsic frame. Theoretical calculations in the deformed shell model suggested the existence of an octupole deformation island around Z = 56 and N = 88 Ce-Ba nuclear region [1, 2]. However, as these nuclei are located in the neutron-rich region, it is difficult to study their high spin states. An efficient method is to measure the prompt γ-rays from fission of the heavy nuclei [3]. Following the development of large detector arrays, much progress has been made in investigating the high spin states in these neutron-rich nuclei. In previous experimental studies, octupole-deformed bands and strong octupole correlations have been observed in many nuclei in this region, especially in Z = 56 Ba and Z = 58 Ce neutron-rich isotopes, such as, in $^{140-146,148}$Ba [3–8], ^{144,146,148}Ce [3, 5, 9–12] by measuring the prompt γ-rays from the spontaneous fission of actinide nuclei.

The very neutron-rich, even-even ^{150}Ce nucleus with Z = 58, N = 92 is located at the edge of the Z = 56, N=88 octupole deformed island. To search for the octupole band structure in this nucleus is important for systematically understanding the characteristics of the octupole correlations in this region. In previous reports [3, 9], only a ground band in ^{150}Ce was identified. In order to extend the levels and to search for evidence of octupole correlations, we re-investigated the level structures of ^{150}Ce. A total of 25 new levels and 47 new transitions are identified. Octupole correlations in this nucleus have been proposed.

II. EXPERIMENT AND RESULTS

The level structure of ^{150}Ce in the present work has been studied by measuring the prompt γ-rays emitted from the fragments produced in the spontaneous fission of ^{252}Cf. The experiment was carried out at the Lawrence Berkeley National Laboratory using a ^{252}Cf source of strength $\sim$ 60 μCi. The source was sandwiched between two Fe foils of thickness of 10 mg/cm^2, and placed at the center of the Gammasphere detector array which, for this experiment, consisted of 101 Compton-suppressed Ge detectors. A total of 5.7×10^{11} triple- and higher fold γ-coincidence events were collected. Thus, these data have higher statistics than our earlier measurements in Refs. [7, 13] by a factor of about 15. Detailed information of the experiment can be found in Refs. [3, 7, 8]. The coincidence data were analyzed with the Radware software package [14] using γ-γ-γ coincidence methods.

A new level scheme of ^{150}Ce obtained in the present

*Electronic address: zhushj@mail.tsinghua.edu.cn

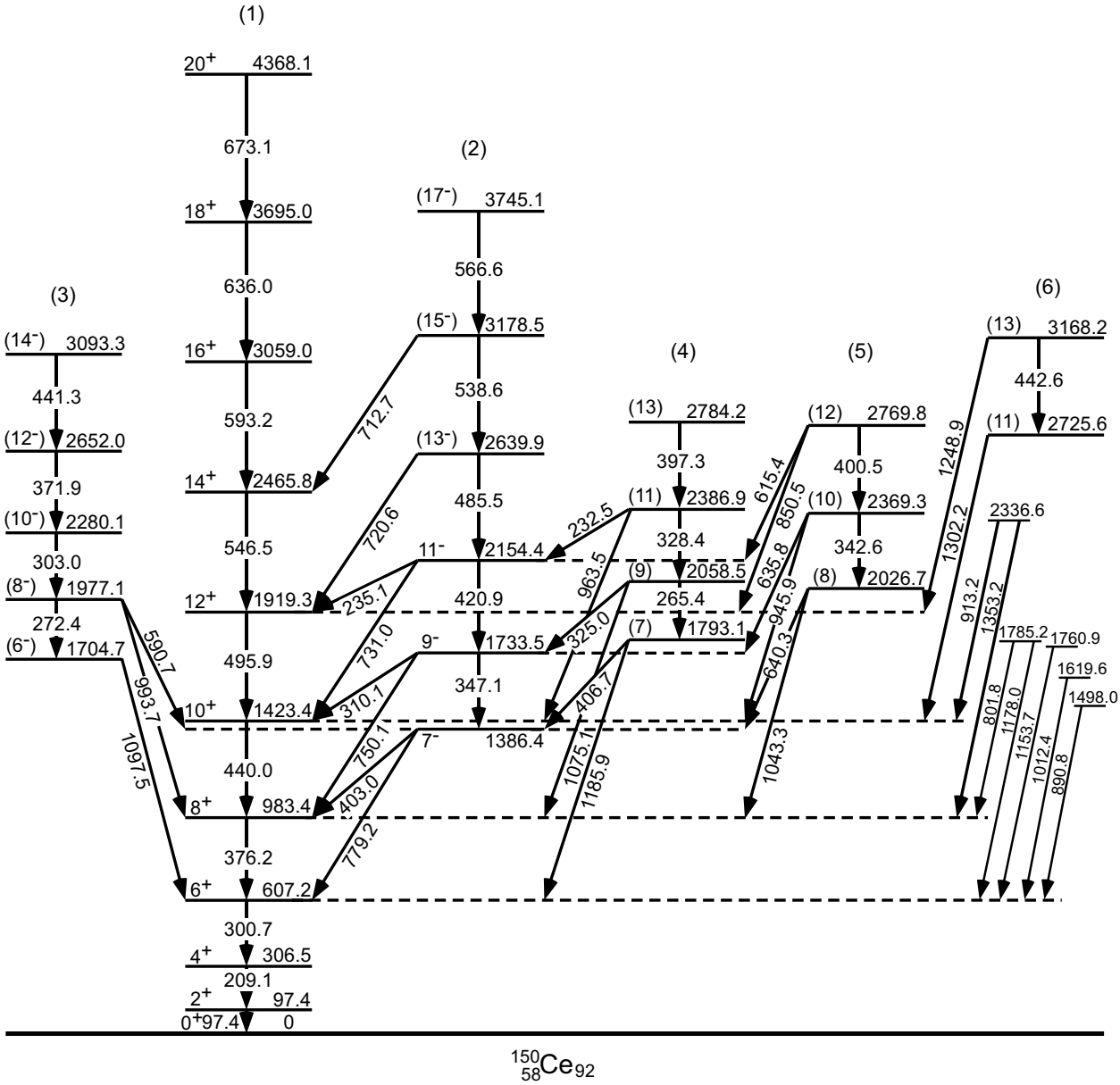

FIG. 1: The level scheme of ^{150}Ce in the present work.

work is shown in Fig. 1. The collective band structures are labeled on top of the bands with numbers (1) - (6) in Fig. 1. They are constructed based on the regular level spaces in each band, the relative transition intensity analysis, and the systematic comparisons with the neighboring nuclei. The results of the analysis are also listed in Table I, including the γ-transition energies, the relative intensities of transitions, and the assignments of spin and parity (I^{π}) values. The γ-transition intensities have been normalized to that of the 209.1 keV ($4^+ \rightarrow 2^+$) γ-ray. Compared to the previous result [3], a total of 47 new transitions and 25 new levels in ^{150}Ce are observed in the present work.

Figs. 2 and 3 give examples of some double-gated γ-ray spectra in ^{150}Ce. In Fig. 2, two γ-ray spectra are obtained by double gating on 209.1 and 300.7 keV transitions of band (1). One can see all the γ-peaks above the 607.2 keV level, including some very weak γ-transitions. In Fig. 3(a) a coincidence spectrum by double gating on 290.1 and 593.2 keV transitions in band (1) is shown. In this spectrum one can clearly see the 97.4, 300.7, 376.2, 440.0, 495.9, 546.5, 636.0 and 673.1 keV γ-transitions in band (1). Fig. 3(b) shows a partial coincidence spectrum with summing double gating on 209.1 and 779.2 keV, and 209.1 and 750.1 keV γ-transitions. In this spectrum, in addition to the strong γ-peaks of 97.4, 300.7 and 376.2 keV in band (1), most of other corresponding coincidence γ-peaks can been seen, such as, 347.1, 420.9, 485.5, 538.6 and 566.6 keV in band (2), 265.4, 328.4 and 397.3 keV in band (4), and 406.7, 325.0 and 232.5 keV between

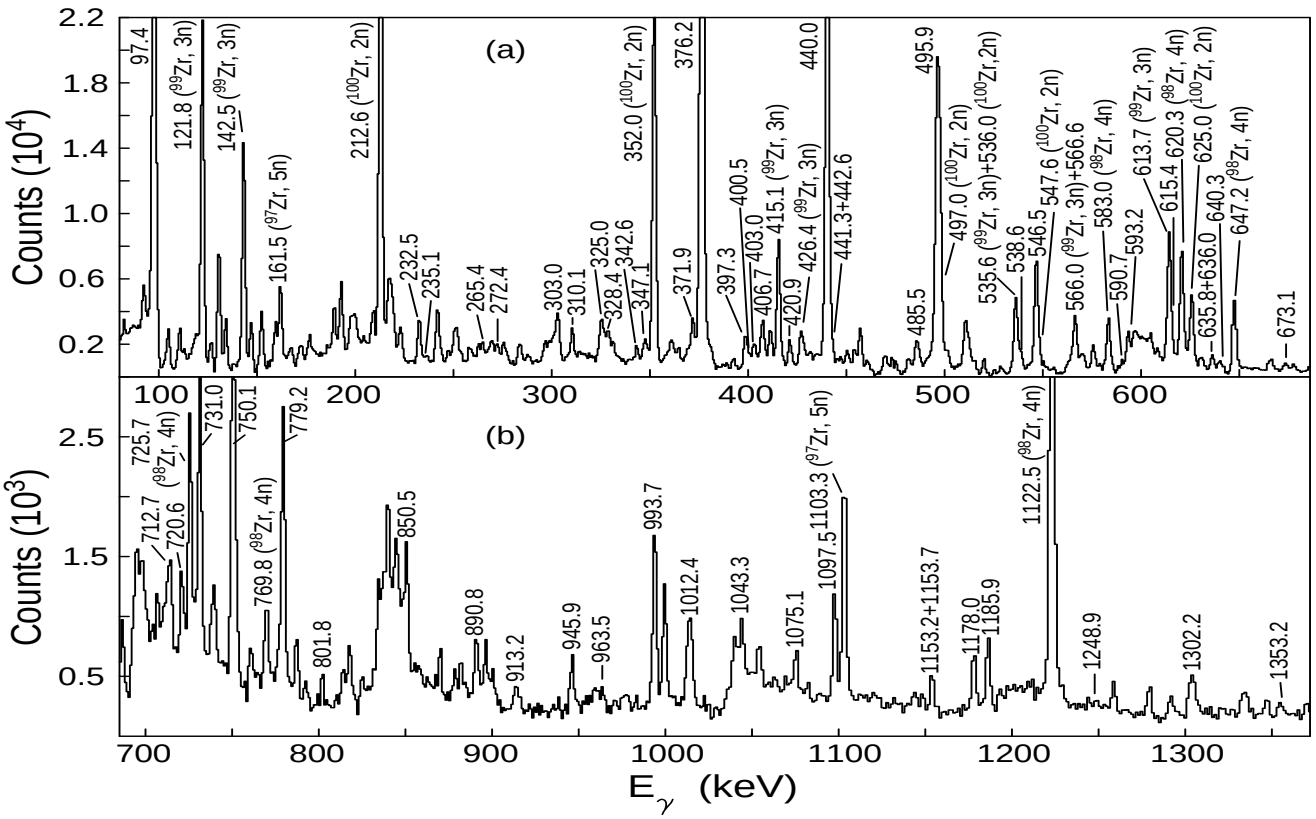

FIG. 2: Partial γ-ray coincidence spectra obtained by double gating on 209.1 and 300.7 keV transitions : (a) the energy covered between 80 and 685 keV, and (b) the energy covered between 685 and 1370 keV in ^{150}Ce. In the spectra, the transitions belonging to Zr partner isotopes are indicated.

bands (2) and (3) etc.. In Fig. 3(c), a coincidence spectrum is given by summing double gating on 300.7 and 1097.5 keV, and 209.1 and 993.7 keV γ-transitions, from which one can see the 272.4, 303.0 (mixed with the 300.7 keV), 371.9 and 441.3 keV γ-peaks in band (2), besides the strong γ-peaks of 97.4, 209.1, 300.7 and 376.2 keV in band (1). In spontaneous fission a pair of correlated partners is produced. By gating on known γ-rays in an isotope, some strong transitions in its correlated partners can be seen. In the present work, the stronger partners of ^{150}Ce are ^{100}Zr(2n), ^{99}Zr(3n), ^{98}Zr(4n) and ^{97}Zr(5n) (numbers in parentheses here indicate the numbers of neutrons emitted after fission). So in the spectra of Figs. 2 and 3, in addition to the peaks belonging to the ^{150}Ce, some partner's peaks, for examples, 212.6, 352.0, 497.0, 536.0, 547.6, 625.0 keV in ^{100}Zr(2n), 121.8, 142.5, 415.1, 426.4, 535.6, 566.0, 613.7 keV in ^{99}Zr(3n), 1222.5, 620.3, 647.2, 583.0, 725.7, 769.8 keV in ^{98}Zr(4n), and 1103.3, 161.5 keV in ^{97}Zr(5n) can be seen.

In the previous publications, the ground band in ^{150}Ce was firstly identified up to 14^+ [9], and then was expanded up to 20^+ [3]. We observed the ground band up to 20^+ as reported in Ref. [3]. Bands (2)-(6) are newly established in the present work. The band (2) is observed from 1386.4 keV up to 3745.1 keV levels. The linking transitions of 779.2, 403.0, 750.1, 310.1, 731.0, 235.1, 720.6 and 712.7 keV between bands (2) and (1) are observed. Through the systematic comparisons with the neighboring nuclei ^{144,146,148}Ce [3, 5, 9–12], we assigned the band (2) as a negative-parity band. So the spins and parities (I^π's) of the band (2) levels are assigned or tentatively assigned as 7^-, 9^-, 11^-, (13^-), (15^-) and (17^-), respectively. Band (3) in ^{150}Ce is built on a 1704.7 keV level. Based on systematic comparison with neighboring isotone ^{152}Nd [15], we tentatively assigned it as a negative parity band and the I^π of the band head level as (6^-). It is difficult to assign the I^π's for the bands (4)-(6) as well as the levels under the band (6) in Fig. 1. We only tentatively assign some spins for bands (4) - (6) as shown in Fig. 1.

In order to have more confirmation for our assignments above, we have carried out $\gamma \rightarrow \gamma(\theta)$ angular correlation measurements based on our data set divided into angular bins [16]. As most of the non-yrast transitions in ^{150}Ce are very weak, we only obtained three angular correlation values of 779.0→300.7, 750.1→376.4 and 731.0→440.1 keV cascades as shown in Fig. 4. The obtained A_2 and A_4 values are -0.065(36) and -0.040(55) for the 779.0→300.7 keV cascade, -0.118(24) and -0.002(38) for the 750.1→376.4 keV cascade, and -0.086(41) and -0.044(63) for the 731.0→440.0 keV cascade, respectively. The theoretical value can be obtained as A_2

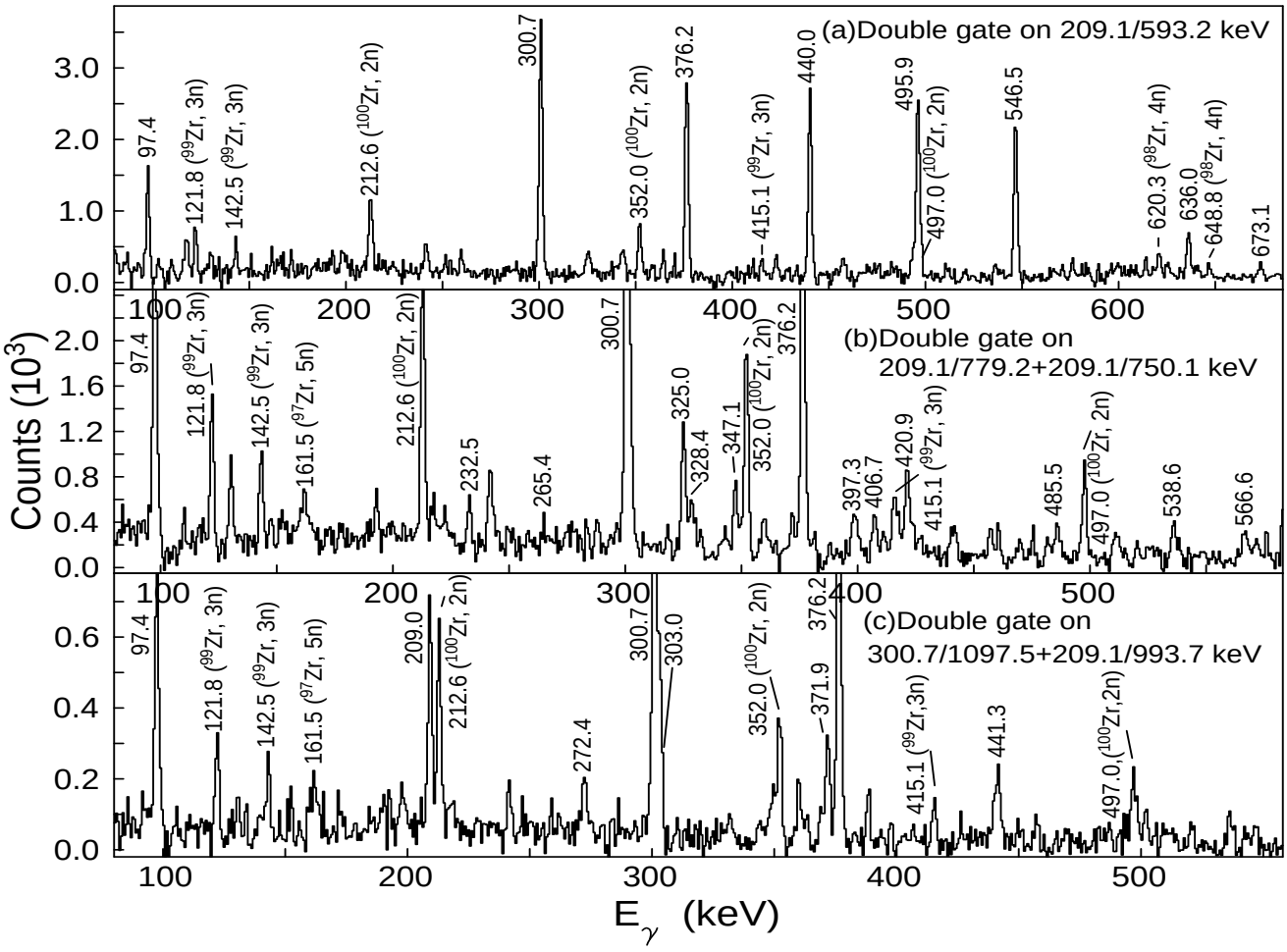

FIG. 3: Partial γ-ray coincidence spectra obtained (a)by double gating on 209.1 and 593.2 keV transitions, (b) by summing double gating on 209.1 and 779.2, and 209.1 and 750.1 keV transitions, and(c) by summing double gating on 300.7 and 1097.5 keV, and 209.1 and 993.7 keV transitions in ^{150}Ce. In the spectra, the transitions belonging to Zr partner isotopes are indicated.

= -0.0714 and A_4 = 0.0 for all the 7^-(E1)6^+(E2)4^+, 9^-(E1)8^+(E2)6^+ and 11^-(E1)10^+(E2)8^+ cascades [17]. These data allow only the spins of 7, 9, and 11 and establish the crossing transitions of 779.0, 750.1, and 731.0 keV between bands (2) and (1) as pure dipole, most probably E1 transitions. Thus the data gives further evidence for our I^π assignments of band (2) in ^{150}Ce.

TABLE I: The energies, relative intensities, multipolarities, and spin and parity (I^π) assignments of the γ-transitions and levels in ^{150}Ce. The $*$ denotes the γ-transition newly identified in this work compared with the results reported in Ref. [3].

E_γ(keV)	Int.(%)	E_i(keV)	→	E_f(keV)	Assignment	Mult.
97.4	49.0(17)	97.4	→	0	$2^+\rightarrow 0^+$	$E2$
209.1	100.0(6)	306.5	→	97.4	$4^+\rightarrow 2^+$	$E2$
$*$232.5	1.47(9)	2386.9	→	2154.4	$(11)\rightarrow 11^-$	
$*$235.1	0.17(3)	2154.4	→	1919.3	$11^-\rightarrow 12^+$	$E1$
$*$265.4	0.53(3)	2058.5	→	1793.1	$(9)\rightarrow(7)$	$(E2)$
$*$272.4	0.95(4)	1977.1	→	1704.7	$(8^-)\rightarrow(6^-)$	$E2$
300.7	86.7(12)	607.2	→	306.5	$6^+\rightarrow 4^+$	$E2$
$*$303.0	2.12(9)	2280.1	→	1977.1	$(10^-)\rightarrow(8^-)$	$E2$

TABLE I: Continue.

E_γ(keV)	Int.(%)	E_i(keV)	→	E_f(keV)	Assignment	Mult.
∗310.1	1.29(7)	1733.5	→	1423.4	9^-→10^+	$E1$
∗325.0	1.54(2)	2058.5	→	1733.5	(9)→9^-	
∗328.4	1.46(13)	2386.9	→	2058.5	(11)→(9)	($E2$)
∗342.6	0.71(6)	2369.3	→	2026.7	(10)→(8)	($E2$)
∗347.1	2.00(15)	1733.5	→	1386.4	9^-→7^-	$E2$
∗371.9	1.20(11)	2652.0	→	2280.1	(12^-)→(10^-)	$E2$
376.2	61.5(5)	983.4	→	607.2	8^+→6^+	$E2$
∗397.3	2.97(41)	2784.2	→	2386.9	(13)→(11)	($E2$)
∗400.5	1.33(29)	2769.8	→	2369.3	(12)→(10)	($E2$)
∗403.0	1.21(7)	1386.4	→	983.4	7^-→8^+	$E1$
∗406.7	1.42(11)	1793.1	→	1386.4	(7)→7^-	
∗420.9	1.59(13)	2154.4	→	1733.5	11^-→9^-	$E2$
440.0	35.9(3)	1423.4	→	983.4	10^+→8^+	$E2$
∗441.3	0.58(7)	3093.3	→	2652.0	(14^-)→(12^-)	$E2$
∗442.6	0.13(2)	3168.2	→	2725.6	(13)→(11)	($E2$)
∗485.5	2.01(13)	2639.9	→	2154.4	(13^-)→11^-	($E2$)
495.9	15.8(3)	1919.3	→	1423.4	12^+→10^+	$E2$
∗538.6	2.02(25)	3178.5	→	2639.9	(15^-)→(13^-)	($E2$)
546.5	7.62(17)	2465.8	→	1919.3	14^+→12^+	$E2$
∗566.6	0.08(2)	3745.1	→	3178.5	(17^-)→(15^-)	($E2$)
∗590.7	0.99(9)	1977.1	→	1386.4	(8^-)→(7^-)	($M1/E2$)
593.2	2.92(12)	3059.0	→	2465.8	16^+→14^+	$E2$
∗615.4	0.67(8)	2769.8	→	2154.4	(12)→11^-	
∗635.8	0.31(4)	2369.3	→	1733.5	(10)→9^-	
636.0	1.12(8)	3695.0	→	3059.0	18^+→16^+	$E2$
∗640.3	0.36(7)	2026.7	→	1386.4	(8)→7^-	
673.1	0.44(5)	4368.1	→	3695.0	20^+→18^+	$E2$
∗712.7	0.90(7)	3178.5	→	2465.8	(15^-)→14^+	($E1$)
∗720.6	1.08(8)	2639.9	→	1919.3	(13^-)→12^+	($E1$)
∗731.0	3.44(13)	2154.4	→	1423.4	11^-→10^+	$E1$
∗750.1	6.64(17)	1733.5	→	983.4	9^-→8^+	$E1$
∗779.2	4.06(11)	1386.4	→	607.2	7^-→6^+	$E1$
∗801.8	0.46(5)	1785.2	→	983.4	→8^+	
∗850.5	1.05(8)	2769.8	→	1919.3	(12)→12^+	
∗890.8	1.24(7)	1498.0	→	607.2	→6^+	
∗913.2	0.17(3)	2336.6	→	1423.4	→10^+	
∗963.5	0.36(4)	2386.9	→	1423.4	(11)→10^+	
∗945.9	1.03(8)	2369.3	→	1423.4	(10)→10^+	
∗993.7	3.14(13)	1977.1	→	983.4	(8^-)→8^+	($E1$)
∗1012.4	2.34(9)	1619.6	→	607.2	→6^+	
∗1043.3	1.61(9)	2026.7	→	983.4	(8)→8^+	
∗1075.1	1.14(8)	2058.5	→	983.4	(9)→8^+	
∗1097.5	2.33(9)	1704.7	→	607.2	(6^-)→6^+	($E1$)
∗1153.7	0.95(7)	1760.9	→	607.2	→6^+	
∗1178.0	1.34(8)	1785.2	→	607.2	→6^+	
∗1185.9	1.58(8)	1793.1	→	607.2	(7)→(6^+)	
∗1248.9	0.46(5)	3168.2	→	1919.3	(13)→12^+	
∗1302.2	0.52(7)	2725.6	→	1423.4	(11)→10^+	
∗1353.2	0.51(5)	2336.6	→	983.4	→8^+	

III. DISCUSSION

Here we mainly discuss the characteristics of the bands (1) and (2) in ^{150}Ce. From Fig. 1, one can see that one set of the positive- and negative-parity bands (1) and (2) with $\Delta I = 2$ transitions in each band and with linking $E1$ transitions between two bands forms an octupole band structure with a simplex quantum number

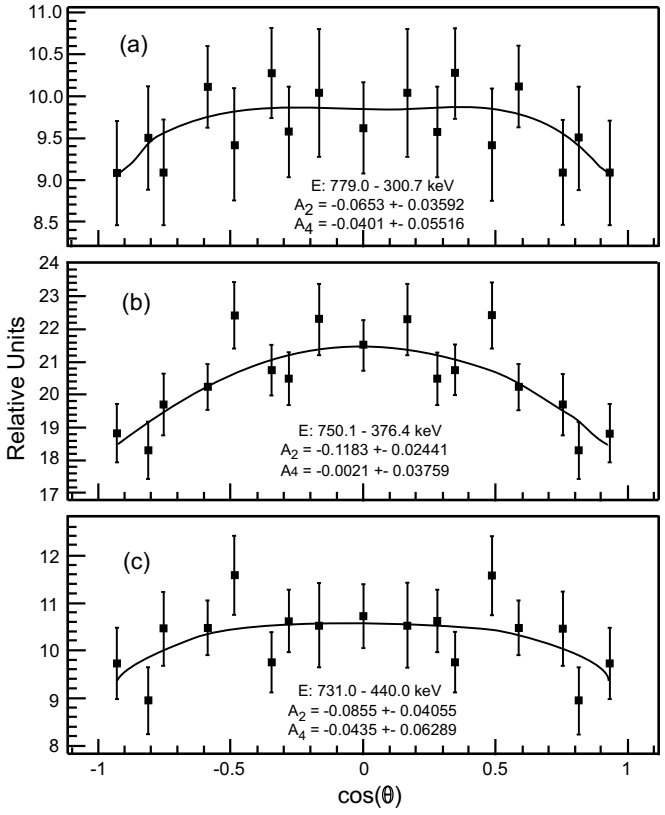

FIG. 4: Angular correlations for (a)779.0→300.7, (b)750.1→376.4 and (c)731.0→440.1 keV cascades in ^{150}Ce.

TABLE II: $B(E1)/B(E2)$ branching ratios in ^{150}Ce.

E_γ(keV)	$I_i^\pi \to I_f^\pi$	I_γ	$\frac{B(E1)}{B(E2)}10^{-6}fm^{-2}$
750.1	$(9^-) \to (8^+)$	6.64	0.031(3)
347.1	$(9^-) \to (7^-)$	2.00	
731.0	$(11^-) \to (10^+)$	3.44	0.056(5)
420.9	$(11^-) \to (9^-)$	1.59	
720.6	$(13^-) \to 12^+$	1.08	0.030(3)
485.5	$(13^-) \to (11^-)$	2.01	
712.7	$(15^-) \to 14^+$	0.90	0.043(7)
538.6	$(15^-) \to (13^+)$	2.02	

$s = +1$. As indicated above, in the earlier publications, the octupole band structures have been observed in the neighboring even-even ^{144,146,148}Ce isotopes [3, 5, 9–12]. Fig. 5 shows a comparison of observed levels in the $s = +1$ octupole structures in ^{144}Ce [10], ^{146}Ce [12], ^{148}Ce [11] and ^{150}Ce (in the present work). They show very similar characters with each other. It indicates that the assigned octupole band structure in ^{150}Ce is reasonable. On the other hand, from Fig. 5 one can see that following the neutron number increasing, the level energies with the same spin systematically decreased. This is caused by the quadrupole deformation (β_2) increasing with the neutron number increasing in these Ce isotopes.

A nucleus with octupole bands decays through $E1$ and $E2$ transitions. The $B(E1)/B(E2)$ branching ratios can been obtained by the expression:

$$\frac{B(E1)}{B(E2)} = 0.771\frac{I_\gamma(E1)}{I_\gamma(E2)}\frac{E_\gamma(E2)^5}{E_\gamma(E1)^3}(10^{-6}\cdot fm^{-2}) \quad (1)$$

where the intensities (I_γ) and energies (E_γ) in ^{150}Ce have been taken from the present work. The $B(E1)/B(E2)$values of the $s = +1$ octupole structure in ^{150}Ce from our investigation are listed in Table [2]. The average $B(E1)/B(E2)$ value for the $s = +1$ octupole structure in ^{150}Ce is 0.040 $\times(10^{-6}\cdot$fm$^{-2})$. The average $B(E1)/B(E2)$ values observed for s = +1 octupole structures in ^{144,146}Ce [10] and ^{148}Ce [11] are 6.12, 1.70, 1.51 $\times(10^{-6}\cdot$fm$^{-2})$, respectively. Observed $B(E1)/B(E2)$ values indicate that the octupole correlations in ^{150}Ce are much weak comparing with the neighboring light Ce isotopes.

In a nucleus with octupole correlations, the energy differences δE between the $\pi = +$ and $\pi = -$ bands can be used to discuss the octupole deformation stability with spin variation. Such δE between the $\pi = +$ and $\pi = -$ bands can be evaluated from the experimental level energies by using the relation [11]:

$$\delta E(I) = E(I^-) - \frac{(I+1)E(I-1)^+ + IE(I+1)^+}{2I+1} \quad (2)$$

Here the superscripts indicate the parities of the levels. Fig. 6 systematically shows plots of the $\delta E(I)$ versus I of the s = +1 octupole band structures in ^{144,146,148,150}Ce. In the limit of stable octupole deformation, $\delta E(I)$ should be close to zero. As seen in Fig. 6, the $\delta E(I)$ decreases with the spin incresing in each Ce isotope. It is near to stable point at I $\sim$ 7 $\hbar$ for ^{144}Ce and at I $\sim$ 9 $\hbar$ for ^{146}Ce, respectively. However, for ^{148,150}Ce, through spin 17 $\hbar$, they still do not reach the stable point. The minimum value $\delta E(I)$ is about 0.15 at I = 13 $\hbar$ for ^{148}Ce, and then the $\delta E(I)$ increases with the spin increasing. For ^{150}Ce, until I = 17 $\hbar$, the $\delta E(I)$ with 0.38 does not reach to the minimum, and still is far from the zero point. On the other hand, at the same spin value, the $\delta E(I)$ value is largest for ^{150}Ce, and next large for ^{148}Ce. This result shows that the octupole correlations become more instable as the neutron number increasing in the neutron-rich Ce isotopes, and it becomes most instable in ^{150}Ce.

Plots of the kinematic moments of inertia (J_1) against the rotation frequencies $\hbar\omega$ for the $s = +1$ octupole structure in ^{150}Ce as well as those in ^{144,146,148}Ce are shown in Fig. 7. In these Ce isotopes, the J_1 values of both positive- and negative-parity bands increase with the neutron number incresing. This is also related to the quadrupole deformation variation. For each Ce isotope, J_1 varies smoothly with increasing spin. Generally the J_1 values in ^{150}Ce have similar characters with these octupole bands in ^{144,146,148}Ce, and agree with the systematics.

Above analysis indicates that in ^{150}Ce the assigned octupole correlations are reasonable, and the observed oc-

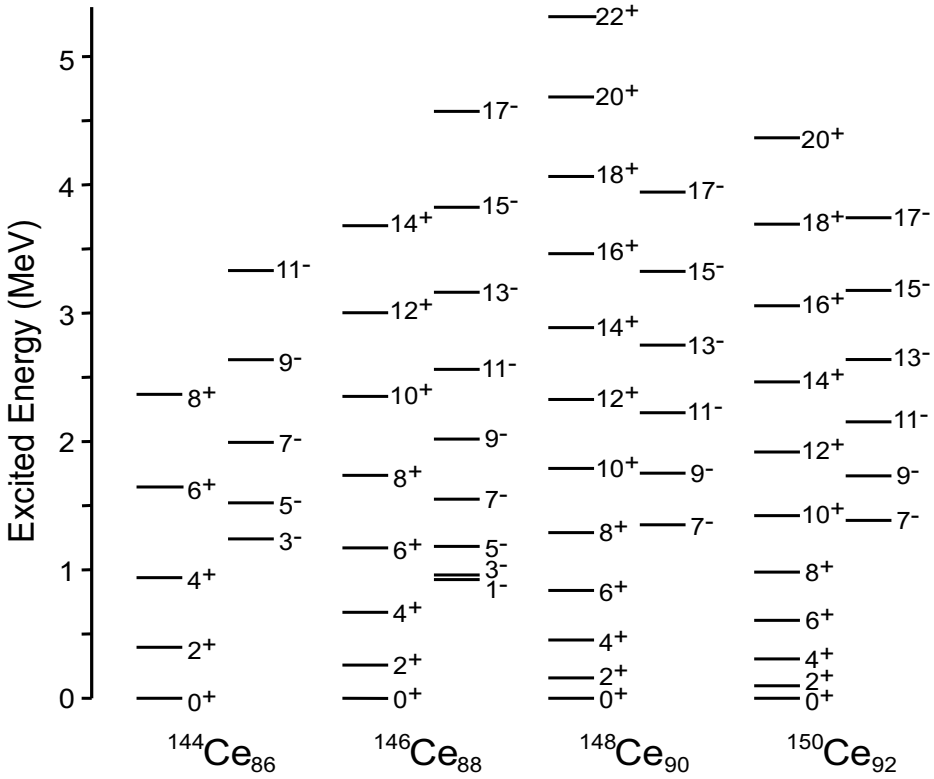

FIG. 5: Systematic comparisons for the levels of $s = +1$ octupole bands in the ^{144}Ce [10], ^{146}Ce [12], ^{148}Ce [11] and ^{150}Ce (in the present work).

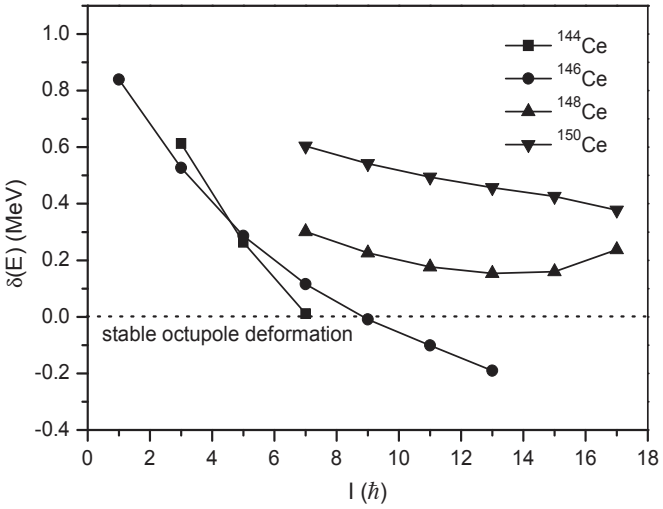

FIG. 6: Plot of $\delta E(I)$ versus spin I for $s = +1$ octupole bands in the ^{144}Ce [10], ^{146}Ce [12], ^{148}Ce [11] and ^{150}Ce (in the present work).

tupole bands are agreement with the systematics. On the other hand, the octupole correlations in ^{150}Ce are weaker and show more instability comparing with the lighter isotopes ^{144,146,148}Ce. This is because the neutron number N = 92 in ^{150}Ce is farther from the N = 88 octupole deformation quantum number by the theoretical prediction in this region. The result shows that ^{150}Ce is indeed located at the edge of Z = 56, N = 88 octupole deformed island. Examining the octupole band structures, the alternating parity levels between the positive- and negative-parity bands have been observed in ^{144,146,148}Ce. But in ^{150}Ce, all the negative-parity levels are higher than the positive parity ones, and no alternating parity levels between the positive- and negative parity bands are observed. This may indicate that the observed negative parity band (2) in ^{150}Ce has the octupole vibrational character.

Band (3) in ^{150}Ce built on the 1704.7 keV level is tentatively assigned as a negative parity band. In ^{152}Nd [15], similar band structure has been assigned as a two quasi-neutron configuration. Based on the structural similarity, band (3) in ^{150}Ce may belong to the two quasi-neutron band also. The characters for the weak bands (4) - (6) as well as several levels below band (6) in ^{150}Ce are not clear, and more work is needed to understand the characters.

IV. SUMMARY

In the present work, the high spin states in ^{150}Ce have been re-investigated. A total of 25 new levels and 47 new transitions are identified, and six collective bands have been observed. An octupole band structure with s = +1 has been proposed. Observed $B(E1)/B(E2)$ branching

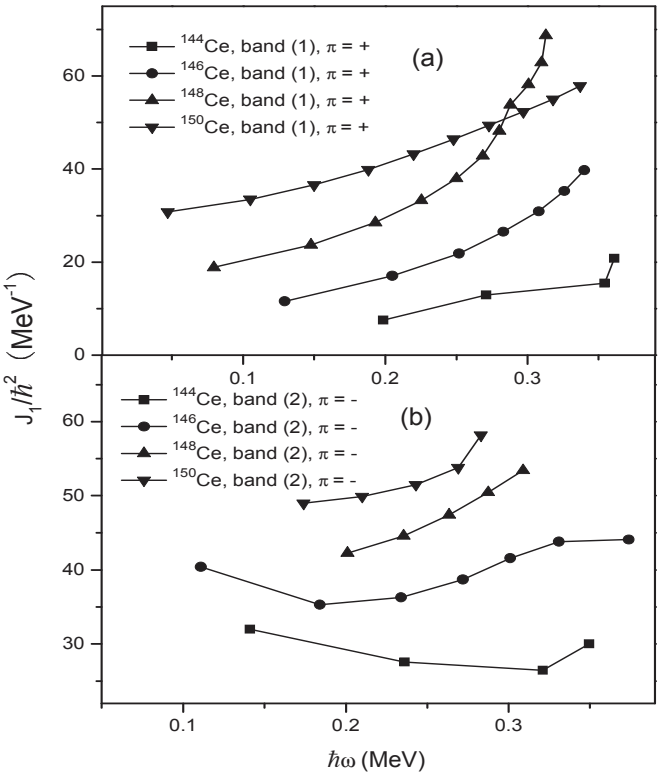

FIG. 7: Moments of inertia (J_1) for (a)positive parity bands and (b)negative parity bands for $s = +1$ octupole bands in the ^{144}Ce [10], ^{146}Ce [12], ^{148}Ce [11] and ^{150}Ce (in the present work).

ratios indicate that the octupole correlations in ^{150}Ce are weaker than that in the lighter Ce isotopes. Other characteristics of octupole correlations in ^{144,146,148,150}Ce are systematically discussed. The result also shows that the negative-parity band in the s = + 1 octupole structure in ^{150}Ce may have an octupole vibrational character.

Acknowledgments

The work at Tsinghua University was supported by the National Natural Science Foundation of China under Grant No.10975082, 11175095, the Special Program of Higher Education Science Foundation under Grant No.2010000211007. The work at Vanderbilt University, Lawrence Berkeley National Laboratory, are supported, respectively, by U.S. Department of Energy under Grant and Contract No. DE-FG05-88ER40407, and DE-AC03-76SF00098. The work at Mississippi State University is support by U.S. Department of Energy under Grant No. DE-FG02-95ER40939.

[1] W. Nazarewicz, P. Olanders, I. Ragnarsson, J. Dudek, G. A. Leander, P. Möller, and E. Ruchowska, Nucl. Phys. A **429**, 269 (1984).

[2] W. Nazarewicz and S. L. Tabor, Phys. Rev. **C 45**, 2226 (1992).

[3] J. H. Hamilton, A. V. Ramayya, S. J. Zhu, G. M. Ter-Akopian, Yu. Ts. Oganessian, J. D. Cole, J. O. Rasmussen, and M. A. Stoyer, Prog. Part. Nucl. Phys. **35**, 635 (1995).

[4] W. R. Phillips, I. Ahmad, H. Emling, R. Holzmann, R. V. F. Janssens, T. L. Khoo, and M.W.Drigert, Phys. Rev. Lett. **57**, 3257 (1986).

[5] S. J. Zhu, Q. H. Lu, J. H. Hamilton, A. V. Ramayya, L. K. Peker, M. G. Wang, W. C. Ma, B. R. S. Babu, T.N. Ginter, J. Kormicki, D. Shi, J.K. Deng, W. Nazarewicz, J. O. Rasmussen, M. A. Stoyer, S.Y. Chu, K.E. Gregorich, M. F. Mohar, S. Asztalos, S. G. Prussin, J. D. Cole, R. Aryaeinejad, Y. K. Dardenne, M. Drigert, K. J. Moody, R. W. Loughed, J. F. Wild, N. R. Johnson, I. Y. Lee, F. K. McGowan, G. M. Ter-Akopian, Yu. Ts. Oganessian, Phys. Lett. B **357**, 273 (1995).

[6] M. A. Jones, W. Urban, J. L. Durell, M. Leddy, W. R. Phillips, A. G. Smith, B. J. Varley, I. Ahmad, L. R. Morss, M. Bentaleb, E. Lubkiewicz, and N. Schulz, Nucl. Phys. **A605**, 133 (1996).

[7] S. J. Zhu, J. H. Hamilton, A. V. Ramayya, E. F. Jones, J. K. Hwang, M. G. Wang, X. Q. Zhang, P. M. Gore, L. K. Peker, G. Drafta, B. R. S. Babu, W. C. Ma, G. L. Long, L. Y. Zhu, C. Y. Gan, L. M. Yang, M. Sakhaee, M. Li, J. K. Deng, T. N. Ginter, C. J. Beyer, J. Kormicki, J. D. Cole, R. Aryaeinejad, M. W. Drigert, J. O. Rasmussen, S. Asztalos, I. Y. Lee, A. O. Macchiavelli, S. Y. Chu, K. E. Gregorich, M. F. Mohar, G. M. Ter-Akopian, A. V. Daniel, Yu. Ts. Oganessian, R. Donangelo, M. A. Stoyer, R. W. Lougheed, K. J. Moody, J. F. Wild, S. G. Prussin, J. Kliman, and H. C. Griffin, Phys. Rev. C **60**, 051304 (1999).

[8] Y. X. Luo, J. O. Rasmussen, J. H. Hamilton, A. V. Ramayya, J. K. Hwang, C. J. Beyer, S. J. Zhu, J. Kormicki, X. Q. Zhang, E. F. Jones, P. M. Gore, T. N. Ginter, K. E. Gregorich, I. Yang Lee, A. O. Macchiavelli, P. Zielinski, C. M. Folden, P. Fallon, G. M. Ter-Akopian, Yu. Ts. Oganessian, A. V. Daniel, M. A. Stoyer, J. D. Cole, R. Donangelo, S. C. Wu, and S. J. Asztalos, Phys. Rev. **C 66**, 014305 (2002).

[9] W. R. Phillips, R. V. F. Janssens, I. Ahmad, H. Emling, R. Holzmann, T. L. Khoo, and M. W. Drigert, Phys. Lett. B **212**, 402 (1988).

[10] L. Y. Zhu, S. J. Zhu , M. Li, J. H. Hamilton, A. V. Ramayya, B. R. S. Babu, W. C. Ma, J. O. Rasmussen, M. A. Stoyer, I. Y. Lee, High Energy Phys. and Nucl. Phys.-Chinese Edition **22**(10), 885 (1997).

[11] Y. J. Chen, S. J. Zhu, J. H. Hamilton, A. V. Ramayya, J. K. Hwang, M. Sakhaee, Y. X. Luo, J. O. Rasmussen, K. Li, I. Y. Lee, X. L. Che, H. B. Ding, and M. L. Li, Phys. Rev. **C 73**, 054316 (2006).

[12] Y. J. Chen, S. J. Zhu, J. H. Hamilton, A. V. Ramayya, J. K. Hwang, Y. X. Luo, J. O. Rasmussen, X. L. Che, H. B. Ding, and M. L. Li, High Energy Phys. and Nucl. Phys.-Chinese Edition **30**(8), 740 (2006).

[13] S. J. Zhu, J. H. Hamilton, A. V. Ramayya, M. G. Wang, J. K. Hwang, E. F. Jones, L. K. Peker, B. R. S. Babu, G. Drafta, W. C. Ma, G. L. Long, L. Y. Zhu, M. Li, C. Y. Gan, T. N. Ginter, J. Kormicki, J. K. Deng, D. T. Shi, W. E. Collins, J. D. Cole, R. Aryaneinejad, M. W. Drigert, J. O. Rasmussen, R. Donangelo, J. Gilat, S. Asztalos, I. Y. Lee, A. O. Macchiavelli, S. Y. Chu, K. E. Gregorich, M. F. Mohar, M. A. Stoyer, R. W. Lougheed, K. J. Moody, J. F. Wild, S. G. Prussin, G. M. Ter-Akopian, A. V. Daniel, and Yu. Ts. Oganessian, Phys. Rev. C **59**, 1316 (1999).

[14] D. C. Radford, Nucl. Instrum. Methods Phys. Res. A **361**, 297 (1995).

[15] E. Y. Yeoh, S. J. Zhu, J. H. Hamilton, A. V. Ramayya, Y. C. Yang, Y. Sun, J. K. Hwang, S. H. Liu, J. G. Wang, Y. X. Luo, J. O. Rasmussen, I. Y. Lee, H. B. Ding, K. Li, L. Gu, Q. Xu, Z. G. Xiao and W. C. Ma, Eur. Phys. J. A **45**, 147 (2010).

[16] A .V. Daniel, C. Goodin, K. Li, A. V. Ramayya, N. J. Stone, J. K. Hwang, J. H. Hamilton, J. R. Stone, Y. X. Luo, J. O. Rasmussen, M. A. Stoyer, S. J. Zhu, G. M. Ter-Akopian, and I. Y. Lee, Nucl. Instrum. Methods B **262**, 399 (2007).

[17] H. W. Taylor, B. Singh, F. S. Prato, and R. McPherson, At. Data Nucl. Data Tables A **9**, 1 (1971).